Eur Radiol (2006) 16: 2603–2611
DOI 10.1007/s00330-006-0212-7

E. M. Coppenrath
U. G. Mueller-Lisse

Multidetector CT of the kidney

Received: 16 November 2005
Revised: 22 January 2006
Accepted: 9 February 2006
Published online: 28 March 2006

E. M. Coppenrath (✉) ·
U. G. Mueller-Lisse
Clinical Radiology,
University of Munich,
Ziemssenstr. 1,
80336 Munich, Germany
e-mail: eva.coppenrath@med.uni-muenchen.de

Abstract The technological development of multidetector CT offers new possibilities for better imaging of organic structures that can be used in diagnosis of the kidney. The thinner slices allow a better spatial resolution, and slice fusion allows improved contrast resolution. The isotropic voxel has been realized in the latest 64-channel scanners. The image quality of arbitrarily reconstructed planes has arrived at the image quality of the scan plane. Faster scanning allows studies in different contrast phases, which is helpful for better discrimination of benign or malignant lesions especially in the highly vascularized kidney. Different phases of contrast uptake can be differentiated (arterial, cortico-medullary, nephrographic, and excretory phase). Multidetector CT brings along the risk of increased dose due to thinner slice collimation and overranging phenomena. Indications for CT investigation of the kidney include urolithiasis, tumor diagnosis and staging, renal trauma, and vascular disease. Even in children, special indications for CT of the kidney remain in polytrauma and tumor staging. Multidetector CT of the kidney has become a very valuable tool in urology, but a careful protocol strategy is mandatory.

Keywords Multidetector CT · Dose reduction · Renal CT protocols

Introduction

Computerized tomography (CT) of the abdomen usually covers the kidneys. This may lead to detection of renal cysts, anatomic variants and even solid masses of the kidneys.

Specific indications for CT investigation of the kidneys include detection of urinary stones, suspicion of renal tumor, tumor staging, diagnosis of renal trauma, vascular disease, and severe infection, such as renal abscess or emphysematous pyelonephritis. An uncomplicated acute infection is not an indication for renal CT. In any case, CT protocols should be tailored to the clinical problem.

Multidetector CT—technological aspects

CT technology has developed rapidly over the past years with 4-, 8-, 16-, 32- and 40-row detector scanners (Table 1). Multidetector CT (MDCT) scanners allow for fast investigation with high spatial resolution [1]. Narrow collimation results in isotropic voxels in 64-channel MDCT scanners of recent release. Images in arbitrarily reconstructed planes come close to the image quality in the original scan plane. Small slice thickness improves the detection of small structures and allows better discrimination of solid and cystic structures as partial-volume effects diminish. Slice fusion options improve contrast and contrast-to-noise ratio.

Due to short scan times, the kidneys can be depicted in well-defined (dynamic) phases of contrast enhancement, so that lesions can be characterized more precisely.

In practice, it is advisable to choose a reconstruction thickness of 3–5 mm as a compromise between spatial resolution and contrast-to-noise ratio. Depending on radiological findings, reconstructions in other planes and slice thickness down to the submillimeter range can be

Table 1 Multidetector CT scanners of latest generation

Scanner	Number of data channels (×mm)	Total detector length *z*-axis (mm)	Gantry rotation time (s)
GE LightSpeed VCT	64×0.625	40	0.35
Philips Brilliance 64	64×0.625	40	0.40
Siemens Sensation 64	64×0.6[a], 24×1.2	28.8	0.37 (0.33 option)
Toshiba Aquilion 64	64×0.5	32	0.40

[a]64×0.6 mm data channels achieved using 32×0.6 mm detectors and *z*-axis flying focal spot

added (depending on scanner type and number of detector rows available).

Multidetector CT increases dose as a result of thinner collimation, overbeaming, and overranging effects. For example, in four-row scanners, effective dose is about 30% higher with a collimation of 1 mm than with a collimation of 2.5 mm. For that reason, and because the interval of breath-holding decreases, a collimation of 2.5 mm is recommended in these scanners. In current multidetector scanners with more than four rows that allow for two different collimations (millimeter and submillimeter), radiation dose increases only by about 10% when the smaller collimation is chosen.

In spiral technique, additional tube rotations have to be performed at the beginning and at the end of the scan range because adjacent data from both sides are necessary for image reconstruction (interpolation). Therefore, the scanned volume exceeds the reconstructed volume. The number of additional rotations depends on pitch, cone beam correction, and scanner type. The overranging effect may cause considerable increase of dose [2].

Dose limitation is possible with the application of dose modulation software. Dose modulation is based on the principle that decrease in body diameter (i.e., the antero-posterior diameter when compared to the lateral diameter) translates into decrease in radiation necessary to obtain a certain contrast-to-noise ratio in the resulting CT image data.

Images are usually reconstructed in the transversal plane. The coronal plane is suitable for reconstruction of an "in situ" perspective that resembles the view of the abdominal or urologic surgeon.

The multiplanar reformation (MPR) describes the option of arbitrary plane reconstruction from voxel data sets. These planes can be chosen in an orthogonal plane (sagittal, coronal), oblique plane or even in a curved planar reconstruction (for example, for course of vessels). Best reconstruction results are obtained in a pseudo-two-dimensional display with isotropic voxels.

Maximum intensity projection (MIP) depicts the structures of highest CT density within a volume of interest. Volume rendering technique (VRT) is an image-processing option that emphasizes regions of selected CT density range [3, 4], thereby accentuating specific tissues or organs.

Investigation protocols

Preparation

To guarantee optimal excretion of contrast media during renal CT, sufficient hydration of the patient is essential. This can be achieved by oral or intravenous administration of fluid volume. However, concomitant disease, such as cardiac or renal insufficiency, has to be considered. Hydration may also minimize nephrotoxic effects of

Table 2 Investigation protocols for the kidney

Parameters	Unenhanced		Portal venous phase	Nephrographic phase	Excretory phase	
Tube voltage (kV)	120		120	120	120	
Pitch	0.9–1.5		0.9–1.5	0.9–1.5	0.9–1.5	
Tube current time product (mAs)	150–200 (S)	30–50 (L)	150–200 (S)	150–200 (S)	150–200 (S)	30–50 (L)
CTDIw (mGy)	12–14 (S)	2–3 (L)	12–14 (S)	12–14 (S)	12–14 (S)	2–3 (L)
Reconstructed slice thickness (mm)	3.0		3.0	3.0	3.0	
Contrast media volume (ml)			120	80–120		
Delay (s)			appr. 70	80–100	appr. 600	
Indications						
Urolithiasis	Low dose		–	–	–	
Renal tumor	Standard dose		–	Standard dose	Low dose	
Ureteral tumor	Standard dose		–	Standard dose	Standard dose	
Pelvic tumor	–		Standard dose	–	Low dose	
Staging	–		Standard dose	–	Low dose	

(*S*) Standard dose, (*L*) low dose

Fig. 1 Horseshoe kidney (4-row multidetector CT)

intravenous contrast media. Simultaneous filling of the gastro-intestinal tract with oral contrast media may be useful. Interfering effects may occur with CT arteriography or CT urography and the application of positive oral contrast media.

Unenhanced CT

Unenhanced CT can be used for the detection of stones within the urinary tract. A low-dose technique may be applied for this indication. In CT protocols including different phases of contrast enhancement (e.g., protocols for tumor characterization) an unenhanced scan is helpful for verification of fat (for instance, in angiomyolipoma or adenoma), detection of blood (increased CT density and lack of contrast enhancement), and detection of calcifications (e.g., complex cystic lesions or renal cell carcinoma).

Contrast enhancement

Imaging of the kidneys in different phases after intravenous contrast media administration depends on sequential arrival of blood carrying contrast media in different parts of the renal parenchyma. Imaging phases have to be selected carefully in accordance with clinical indication (Table 2).

The arterial CT phase is reached about 20–30 s after commencement of intravenous contrast media injection (for renal arteriography, a contrast bolus of 3.5 ml/s is desirable). Alternatively, a test bolus scan or a bolus tracking program can be applied for optimal start of the arterial scan. In the arterial phase, renal arterial stenosis or evaluation of stent implantation can be judged, and acute bleeding can be detected or ruled out.

The cortico-medullary CT phase (about 30–70 s after i.v. contrast) shows high contrast in the renal cortex. Early opacification of renal veins is also detectable. The renal medulla demonstrates with low contrast. The cortico-medullary phase is suitable for depiction of vascular renal anatomy (aneurysm, arteriovenous malformation, fistula) [5]. If a solid lesion appears hyperdense in this phase, it has to be considered to be malignant because renal cell carcinoma is often hypervascularized. Nevertheless, the cortico-medullary phase is not mandatory for the tumor protocol (Table 2), since the nephrographic phase is more sensitive for tumor detection [6–9].

The nephrographic CT phase (80–120 s) shows renal cortex and medulla with equal enhancement. Solid renal lesions usually appear hypodense. This phase is recommended for tumor detection [8]. For optimization of nephrographic phase imaging, some authors prefer the bolus-tracking technique [10].

The excretory CT phase (more than 180 s after intravenous contrast media administration) shows the opacified renal pelvis, ureter and urinary bladder (complete filling of the urinary bladder with contrast media usually takes about 20 min). Optimal time delay of ureteral filling has been reported to be about 10–15 min [11]. Wall thickening of renal pelvis or ureter, or tumor extension into the renal pelvis presents as a hypodense filling defect that stands out against the contrast media within the lumen of the urinary tract. Substantial dose reduction currently cannot be recommended in cases of intrinsic urinary tract lesions.

If the excretory CT phase is performed additionally in the tumor-staging protocol when obstruction of the urinary tract from the outside is suspected, substantial dose reduction may be reasonable. As a supporting technique, prone positioning of the patient and compression of the kidneys for better depiction of the ureters have been discussed [12–14]. The application of furosemide was

Fig. 2 Bosniak cyst type IV on the right side, status post nephrectomy on the left side (64-row MDCT)

Fig. 3 **a** Cyst with hemorrhage (unenhanced axial scan) (4-row MDCT). **b** Cyst with hemorrhage and cyst with small septum (Bosniak II cysts in cortico-medullary phase of contrast enhancement, 4-row MDCT)

reported as a valuable measure [15, 16]. In MDCT a relatively small volume of contrast media (30 ml) may be sufficient for a good calyceal visualization [17].

In consideration of five distinct phases of renal CT, a selection has to be made for clinical indications to avoid accumulation of dose [18]. Effective dose was measured about 15 mSv for CT urography. Effective dose can vary depending on the number of abdominal scans [19].

In split bolus technique, intravenous contrast media is applied at two different time points (e.g., with an interval of 10 min) before a single CT scan of the kidneys and urinary tract is obtained. The urinary tract is opacified with excreted contrast media from the first bolus when the scan commences after the second bolus of contrast media. If the scan is started such that there is a delay of 80–120 s after commencement of the second bolus, the kidneys are depicted in the nephrographic phase, while the renal collecting systems and the ureters are depicted in the excretory phase. Therefore, only one scan is necessary for investigating two contrast media phases [13, 20].

For investigation of children, MRI appears more suitable in most cases [21, 22]. However there are rare indications that require rapid action, such as polytrauma. In this case, dose reduction can be adjusted to noise or body weight [21, 23, 24]. Tumor staging of nephroblastoma by means of CT has been proven to be reasonable in children [25].

Renal disease

Anatomic anomalies and variations

Unilateral renal agenesis, renal duplication, ureter duplex, ureter fissus, horseshoe kidney (Fig. 1) [26] or pancake kidney, minor malrotation (with slight ventralization of pelvis) are chance findings in abdominal CT performed for other clinical indications [27, 28]. Fetal lobulation of the kidney persists frequently in children, but rarely in adults [29]. The reconstruction in other planes, especially in the coronal plane, is helpful for exact anatomic location. A specific renal CT protocol is usually not necessary. A low-dose excretory CT phase improves delineation of a ureteral variant (e.g., exact anatomic situation of a ureter fissus). Vascular anomalies, such as accessory renal arteries or atypical arterial or venous branches, should always be described as a radiological finding.

Table 3 Bosniak classification of renal cysts

Bosniak category	Malignancy	Features
I	Benign	Hairline thin wall, no septa, no calcification, no contrast enhancement, no solid components, cyst content with water density
II	Probably benign	Hairline thin wall, few hairline thin septa, fine calcification, no contrast enhancement, no solid components, cyst content >20 HU
II F	Probably benign	More hairline thin septa, minor contrast enhancement, nodular calcifications, no solid components, cyst content >20 HU
III	Malignant in approximately 30% of cases = potentially malignant	Indeterminate cystic masses, irregular thickened wall, irregular septa, contrast enhancement, no solid components
IV	Malignant	Clearly malignant cystic lesions, contrast enhancement, solid components

Cystic renal masses

Solitary renal cysts are found frequently and do not have pathological significance. The criteria of an uncomplicated cyst that does not need follow-up are water-like CT density, no contrast enhancement (<10 HU), no septa, no solid parts, no rim enhancement, no calcification. Solitary renal cysts are generally classified according to Bosniak (Table 3, Fig. 2) [30, 31].

A cyst with hemorrhage (Fig. 3a and b) may be suspected to represent a solid lesion when no unenhanced scan has been performed. Such a cyst has a CT density of approximately 40–60 HU (>20 HU). Contrast opacity or hemorrhage cannot be differentiated by contrast-enhanced CT.

An infected cyst may show increased CT density values (about 20–30 HU) without contrast enhancement in the central liquid part. However rim enhancement is frequent in case of abscess.

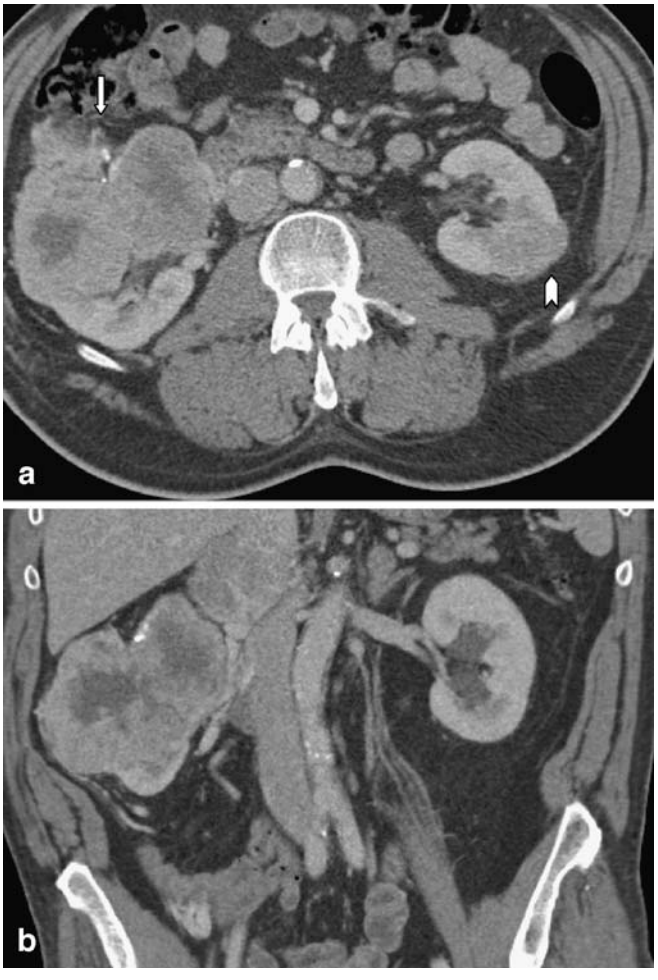

Fig. 4 a,b 64-row MCDT. **a** Bilateral renal cell carcinoma. *Right* Large, dumbbell-shaped tumor with irregular anterior margin (*arrow*), implying extracapsular extension (T3a). *Left* Small, latero-posterior tumor with smooth contour (*arrowhead*), implying restriction to the renal capsule (T1). **b** Renal cell carcinoma with tumor thrombus extending into the inferior v. cava

Fig. 5 Small urothelial carcinoma on the left side (*arrow*) presenting as a low-density lesion outlined on three sides by high-density urine with excreted contrast media in the excretory phase of renal CT (4-row MDCT)

Polycystic kidneys have to be judged carefully. The cysts often show with septa, hemorrhage of different age, or calcifications. Small, solid contrast-enhancing parts have to be suspected to be malignant.

The classification of Potter describes congenital anomalies of the kidneys with predominantly polycystic malformations. Even unilateral and bilateral agenesis of the kidney is described by this classification. CT investigations of adults may reveal the adult form of polycystic disease (Potter type III) with autosomal dominant trait. Cysts often demonstrate hemorrhage (in about 70%) and calcifications

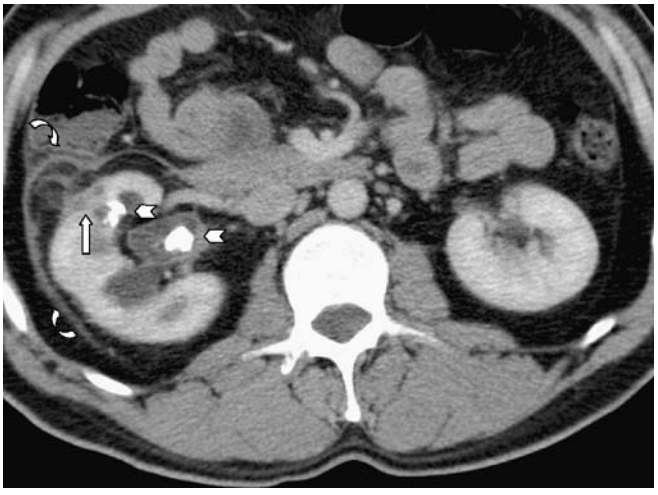

Fig. 6 Renal abscess (*arrow*), kidney stones (*arrowheads*) in infectious complication of calculus disease with severe pyelonephritis. Note inflammatory thickening of Gerota's fascia and Zuckerkandl's fascia (*curved arrows*) (4-row MDCT)

Fig. 7 Pyelonephritis with wedge-shaped hypodense areas (*arrow*) of delayed contrast enhancement in the nephrographic phase of renal CT imaging (4-row MDCT)

(<50%). However the incidence of malignancy is not elevated [3].

Polycystic kidneys can be found in von Hippel-Lindau syndrome. Small, contrast-enhancing solid parts have to be considered to be angioblastoma or renal cell carcinoma (increased risk of approximately 35%, often bilateral or multicentric) [3]. Long-time dialysis is a reason for acquired polycystic kidneys with increased risk of renal cell carcinoma [32].

Solid tumors

Oncocytoma

Oncocytomas are benign tumors (3–5% of all renal tumors). The typical spoke-wheel pattern is characteristic, but the discrimination from renal cell carcinoma is not possible in all cases [3, 33].

Angiomyolipoma

Angiomyolipoma is a benign hamartosis. Angiomyolipoma consists of atypical muscle fibers, blood vessels and fat tissue [3]. If a solid lesion reveals CT density values of fat, angiomyolipoma is highly probable. Only if the fatty regions are very small [34] or the solid part is growing in follow-up investigations, must renal cell carcinoma be considered as a differential diagnosis. Calcifications may indicate malignant tumors. Angiomyolipoma of the kidneys can be associated with lymphangioleiomyomatosis of the lung and with tuberous sclerosis (Bourneville-Pringle syndrome).

Renal cell carcinoma

Renal cell carcinoma (Fig. 4a and b) is the most frequent malignant tumor of the kidney (3% of all adult neoplasms) [40]. The prognosis of T1 or T2 tumor is very good. About one-third of all tumors are reported to be found by chance [3]. Reports vary from approximately 25–50% [35–38]. CT of the abdomen performed for other reasons sometimes detects small, solid renal lesions that suggest renal cell carcinoma.

Renal cell carcinoma is most frequently hyperdense in the cortico-medullary phase, and hypodense in the nephrographic phase.

The nephrographic phase can define tumorous areas in most cases. Studies have shown that specificity and accuracy increase when both phases are combined. During tumor staging, tumor thrombus in the renal vein or v. cava has to be considered [41]. Multidetector-row CT and MR imaging

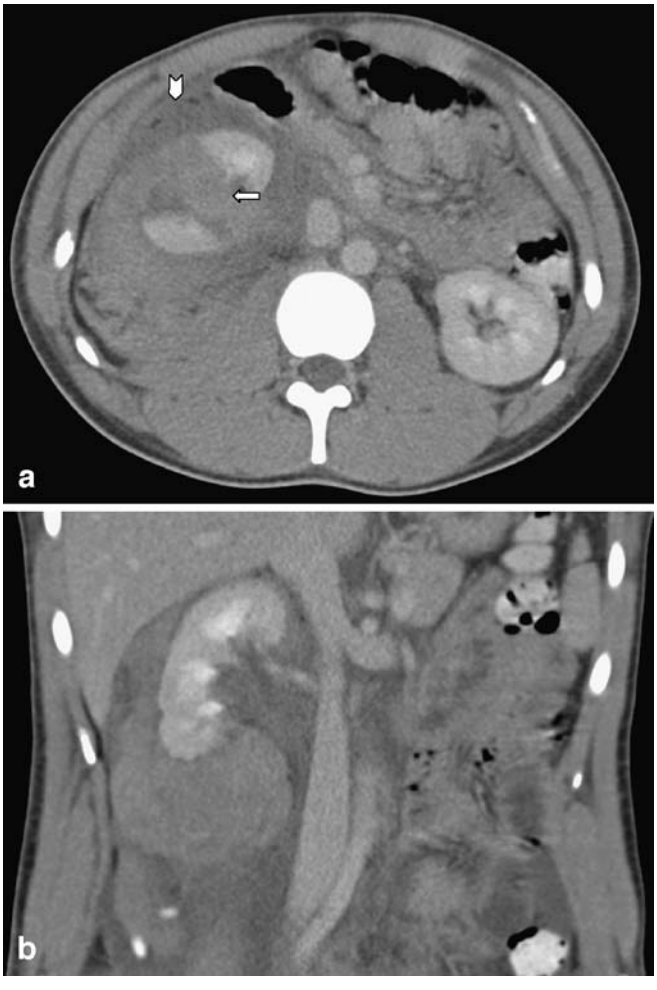

Fig. 8 a,b 16-row MDCT. **a** Renal trauma with extensive retroperitoneal bleeding. Note right-sided renal parenchymal fracture (*arrow*) and perirenal and pararenal hematoma with anterior bulging of Gerota's fascia (*arrowhead*) and anterior displacement of renal fragments. **b** Coronal plane of renal trauma (same patient)

achieve similar accuracy in tumor staging of renal cell carcinoma [42]. A better differentiation of T2 and T3a tumors (perirenal fat infiltration) is decisive for surgical procedure (nephron sparing surgery or radical nephrectomy) [43].

Urothelial carcinoma (transitional cell carcinoma)

Tumors of the renal pelvis and ureter (Fig. 5) can be detected by CT. A CT protocol in the excretory phase with a slice thickness of 3 mm is useful. Structures of soft-tissue density bulge against the hyperdense renal pelvis, or the wall may be partially thickened. MPR is recommended for detection of multicentric lesions [39]. Radiation dose should not be selected too low in order to guarantee sure tumor detection for most with weight or body-mass-index adaptation.

Inflammatory diseases of the kidney

Suspicion of renal abscess (Fig. 6) can be an indication for CT investigation. Liquid parts show increased CT density values (10–30 HU). Inclusion of gas implies a serious complication of infection with gas-producing bacteria. Fungus disease may show microabscesses that may calcify.

Pyonephrosis is an infection of an entire kidney that is affected by hydronephrosis. The renal parenchyma reveals hypodense CT values, while the renal pelvis is filled with pus and urine and demonstrates with low positive CT density (10–50 HU). CT signs of renal tuberculosis are not specific. Abscesses and calcifications can be detectable.

Xanthogranulomatous pyelonephritis is a chronic inflammation of the kidney secondary to urinary obstruction. Parenchymal calcifications and calculi in the pelvis are frequent findings. The affected kidney is mostly enlarged with hypodense areas that correspond with debris and xanthomatous cells. Differential diagnosis is tumor mass [3].

The uncomplicated urinary tract infection is no CT indication [44]. Nevertheless, it can be found in a routine abdominal CT by chance and should be detected correctly. Wedge-shaped focal areas appear slightly hypodense in the nephrographic phase (Fig. 7). CT morphology may be similar to tumor. Differentiation from abscesses is necessary.

Renal trauma

Haematoma

Polytraumatized patients are usually investigated by means of abdominal CT after intravenous contrast enhancement (generally, in the portal-venous phase, with a slice thickness of 5 mm). Renal injury can be detected with this protocol [45, 46].

Renal haematoma can present as a retroperitoneal mass (subcapsular, perirenal, pararenal) (Fig. 8a and b) deriving from the kidney. The CT density is typically about 60 HU. Active bleeding may lead to contrast enhancement within the haematoma and reach tremendous extents, spreading over the whole retroperitoneal space.

Injury of renal pelvis or ureter

Free fluid is apparent and is usually located in the retroperitoneum. The injury of the urine-collecting system can be shown in the excretory phase due to extravasation of contrast-enhanced urine into the retroperitoneum.

Rupture or injury of the renal hilum demonstrates with unilaterally devascularized kidney or contrast deposit at the renal hilum.

Urolithiasis

Unenhanced CT has evolved as a well-accepted alternative to intravenous urography in patients with suspicion of urolithiasis [47, 48]. Higher diagnostic accuracy and better economic impact have been reported [49]. Numerous authors have confirmed that unenhanced scans of the kidney and urogenital organs can be performed for detection of calcified stones with considerably reduced dose [50–53]. Three-dimensional reconstruction allows for highly accurate determination of the volume of renal calculi [54]. It has been reported that the soft-tissue "rim" sign is helpful for differentiation between ureteral stones and phleboliths [55].

Renal vascular disease

Renal artery stenosis is a rather common finding. CT is helpful for follow-up of interventional treatment (balloon dilatation or stent implantation). Spontaneous renal artery dissection can be revealed by helical CT angiography [56].

Conclusion

MDCT offers manifold advantages for image quality in comparison with single slice CT. The realization of isotropic voxels allows reconstruction in arbitrary planes and in three spatial dimensions. This may be beneficial for detection of small tumorous lesions, or for individual surgical planning. Solid lesions and cysts are better judged by means of multidetector CT, with partial volume effects being diminished but not abolished. Temporal resolution is

also improved due to faster tube rotation and greater detector length. Different phases of contrast enhancement can be selected, which is especially valuable for characterization of solid renal lesions.

MDCT carries the risk of dose accumulation with increasing number of scans (different contrast media phases). CT protocols have to be tailored to clinical indication. Individual CT phases (e.g. unenhanced or excretory phase) can be performed in low-dose technique. The application of contrast media should be handled carefully; accumulative nephrotoxic effects may occur over a lifetime. The growing age and comorbidity of patients and complex comedication will become more important in the future [57].

References

1. Foley WD (2003) Renal MDCT. EJR 45:S73–S78
2. Tzedakis A, Damilakis J, Perisinakis K, Statakis J, Gourtsoyiannis N (2005) The effect of z overscanning on patient effective dose from multidetector helical computed tomography examinations. Med Physic 32:1621–1629
3. Schaefer-Prokop C, Prokop M (2003) Kidneys. In: Prokop M, Galanski M (eds) Spiral and multislice computed tomography of the body. Thieme, Stuttgart, pp 639–681
4. Kemper J, Adam G, Nolte-Ernsting C (2005) Multislice CT urography: aspects for technical management and clinical application. Radiologe 45:905–914
5. Yuh BI, Cohan RH (1999) Different phases of renal enhancement: role in detection and characterizing renal masses during helical CT. AJR 173:747–755
6. Cohan RH, Sherman LS, Korobkin M, Bass JC, Francis IR (1995) Renal masses: assessment of corticomedullary-phase and nephrographic-phase CT scans. Radiology 196:445–451
7. Szolar DH, Kammerhuber F, Altziebler S, Tillich M, Breinl E, Fotter R, Schreyer HH (1997) Multiphasic helical CT of the kidney: increased conspicuity for detection and characterization of small (<3 cm) renal masses. Radiology 202:211–217
8. Mueller-Lisse UG, Mueller-Lisse UL (2004) Multi-detector CT of the kidneys. In: Multislice CT, 2nd revised edition. Medical radiology - diagnostic imaging. Springer, Berlin Heidelberg New York, pp 211–232
9. Sheth S, Scatarige JC, Horton KM, Corl FM, Fishman FK (2001) Current concepts in the diagnosis and management of renal cell carcinoma: role of multidetector CT and three-dimensional CT. Radiographics 237–254
10. Birnbaum BA, Jacobs JE, Langlotz CP, Ramchandani P (1999) Assessment of a bolus-tracking technique in helical renal CT to optimize nephrographic phase imaging. Radiology 211:87–94
11. Meindl T, Coppenrath E, Khalil R, Mueller-Lisse UL, Reiser M, Mueller-Lisse UG (2006) MDCT-urography: retrospective determination of optimal delay time after intravenous contrast administration. Eur Radiol (in press)
12. McTavish JDJM, Zou KH, Nawfell RD, Silverman SG (2002) Multi-detector row CT urography: comparison of strategies for depicting the normal urinary collecting system. Radiology 225:783–790
13. Chow LC SF (2001) Multicenter CT urography with abdominal compression and three-dimensional reconstruction. AJR 177:849–855
14. Caoilli EM, Inampudi P, Cohan RH, Ellis JH (2005) Optimization of mulitidetector row CT urography: effect of compression, saline administration, and prolongation of acquisition delay. Radiology 235:116–123
15. Nolte-Ernsting C, Staatz G, Wildberger J, Adam G (2003) MR-urography and CT-urography: principles, examination techniques, applications. RöFo Fortschr Röntgenstr 175:211–222
16. Kemper J, Regier M, Begemann PG, Stork A, Adam G, Nolte-Ernsting C (2005) Multislice computed tomography: intraindividual comparison of different preparation techniques for optimized depiction of the upper urinary tract in an animal model. Invest Radiol 40:126–133
17. Raptopoulos V, McNamara A (2005) Improved pelvicalyceal visualization with multidetector computed tomography urography; comparison with helical computed tomography. Eur Radiol 15:1834–1840
18. Dahlmann P, Semenas E, Brekkan E, Bergman A, Magnusson A (2000) Detection and characterization of renal lesions by multiphasic helical CT. Acta Radiol 41:361–366
19. Nawfel RD, Judy PH, Schleipman AR, Silverman SG (2004) Patient radiation dose at CT urography and conventional urography. Radiology 232:126–132
20. McNicholas MMJ, Raptopoulos V, Schwartz RK, Sheiman RG, Zormpala A, Prassapoulos, PK, Ernst RD, Pearlman JD (1998) Excretory phase CT urography for opacification of the urinary collecting system. AJR 170:1261–1267
21. Puig S, Schaefer-Prokop C, Mang T, Prokop M (2002) Single- and multislice spiral computer tomography of the paediatric kidney. EJR 43:139–145
22. Riccabona M (2003) Imaging of renal tumours in infancy and childhood. Eur Radiol 13(Suppl L):116–129
23. Jangland L, Sanner E, Persliden J (2004) Dose reduction in computed tomography by individualized scan protocols. Acta Radiol 45:301–307
24. Coppenrath E, Schmid C, Brand R, Szeimies U, Hahn K (2001) Spiral CT of the abdomen: weight-adjusted dose reduction. RöFo Fortschr Roentgenstr 173:52–56
25. Olsen OE, Jeanes AC, Sebire NJ, Roebuck DJ, Michalski AJ, Risdon RA, Owens CM (2004) Changes in computed tomography features following preoperatvie chemotherapy for nephroblastoma: relation to histopathological classification. Eur Radiol 14:990–994
26. Kehagias DT, Gouliamos AD, Vlahos LJ (1999) Horseshoe kidney associated with anomalous inferior vena cava. Eur Radiol 9:935–936
27. Barbaric ZL (1994) Principles of genitourinary radiology, 2nd edn. Thieme, New York
28. Cocheteux BM, Mounier-Vehier C, Gaxotte V, McFadden EP, Francke JP, Beregi JP (2001) Rare variations in renal anatomy and blood supply: CT appearance and embryological background. A pictorial essay. Eur Radiol 11:779–786
29. Campbell MF (1970) Anomalies of the kidney. In: Campbell MF, Harrison JH (eds) Urology, vol 2, 3rd edn. Saunders, Philadelphia, p 1416
30. Bosniak MA (1997) Diagnosis and management of patients with complicated cystic lesions of the kidney. AJR 169:819–821

31. Warren KS, McFarlane (2004) The Bosniak classification of renal cystic masses. BJU 95:939–942
32. Choyke PL (2000) Acquired cystic kidney disease. Eur Radiol 10:1716–1721
33. Tunaci A, Yekeler E (2004) Multidetector row CT of the kidneys. Eur J Radiol 52:56–66
34. Obuz F, Karabay N, Secil M, Igci E, Kovanlikaya A, Yorukoglu K (2000) Various radiological appearances of angiomyolipomas in the same kidney. Eur Radiol 10:897–899
35. Konnak JW, GrossmanHB (1985) Renal cell carcinom as an incidental finding. J Urol 134:1094–1096
36. Lanctin HP, Futter NG (1990) Renal cell carcinoma: incidental detection. Can J Surg 33:488–490
37. Rauschmeier H (1986) Sonography - the most important study in the early detection of renal cell carcinoma. Urologe A 25:325–328
38. Tsukamoto T, Kumamoto Y, Yamazaki K, Miyao N, Takahashi A, Masumori N, Satoh M (1991) Eur Urol 19:109–113
39. Rimondini A, Morra A, Bertolotto M, Locatelli M, Pozzi Mucelli R (2001) Radiol Med (Torrino) 101:459–465
40. Sokoloff MH, de Kernion JB, Figlin RA, Belldegrun A (1996) Current management of renal cell carcinoma. CA Cancer J Clin 46:284–302
41. Hallscheidt PJ, Fink C, Haferkamp A, Bock M, Luburic A, Zuna I, Noeldge G, Kaufmann G (2005) Preoperative staging of renal cell carcinoma with inferior vena cava thrombus using CT and MRI: prospective study with histopathological correlation. J Comput Assist Tomogr 29:64–68
42. Hallscheidt PJ, Bock M, Riedasch G, Zuna I, Schoenberg S, Autschbach F, Soder M, Noeldge G (2004) Diagnostic accuracy of staging renal cell carcinomas using multidetector-row computed tomography and magnetic resonance imaging: a prospective study with histopathologic correlation. J Comput Assist Tomogr 28:333–339
43. Catalano F, Fraioli F, Laghi A, Napoli A, Pediconi F, Danti M, Nardis P, Passariello R (2003) High-resolution multidetecto CT in the preoperative evaluation of patients with renal cell carcinoma. AJR 180:1271–1277
44. Browne RF, Zwirewich C, Torreggiani WC (2004) Imaging of urinary tract infection in the adult. Eur Radiol 14 (Suppl 3):E168–E183
45. Harris AC, Zwirewich CV, Lyburn ID, Torreggiani WC, Marchinkow LO (2001) CT findings in blunt renal trauma. Radiographics 21:S201–S214
46. Kawashima A, Sandler CM, Corl FM, West OC, Tamm EP, Fishman EK, Goldman SM (2001) Imaging of renal trauma: a comprehensive review. Radiographics 21:557–574
47. Tamm EP, Silverman PM, Shuman WP (2003) Evaluation of the patient with flank pain and possible ureteral calculus. Radiology 228:319–329
48. Heneghan JP, McGuire KA, Leder RA, DeLong DM, Yoshizumi T, Nelson RC (2003) Helical CT for nephrolithiasis and ureterolithiasis: comparison of conventional and reduced radiation-dose techniques. Radiology 229:575–580
49. Pfister SA, Deckart A, Laschke S, Dellas S, Otto U, Buitrago C, Roth J, Wiesner W, Bongartz G, Gasser TC (2003) Unenhanced helical computed tomography vs intravenous urography in patients with acute flank pain: accuracy and economic impact in a randomized prospective trial. Eur Radiol 13:2513–2520
50. Spielmann AL, Heneghan JP, Lee LJ, Yoshizumi T, Nelson RC (2002) Decreasing the radiation dose for renal stone CT: a feasibility study of single- and multidetector CT. AJR 178:1058–1062
51. Tack D, Sourtzis S, Dellpierre I, de Maertelaer V, Genenois PA (2003) Low-dose unenhanced multidetector CT of patients with suspected renal colic. AJR 180:305–311
52. Hamm M, Knöpfle E, Wartenberg S, Wawroschek F, Weckermann D, Harzmann R (2002) Low dose unenhanced helical computerized tomography for the evaluation of acute Flank pain. J Urol 167:1687–1691
53. Rimondini A, Pozzi Mucelli R, De Denaro M, Bregant P, Dalla Palma L (2001) Evaluation of image quality and dose in renal colic: comparison of different spiral-CT protocols. Eur Radiol 11:1140–1146
54. Olcott EW, Sommer FG, Napel S (1997) Accuracy of detection and measurement of renal calculi: in vitro comparison of three-dimensional spiral CT, radiography and nephrotomography. Radiology 204:19–25
55. Heneghan JP, Dalrymple NC, Verga M, Rosenfield AT, Smith RC (1997) Soft-tissue "rim" sign in the diagnosis of ureteral calculi with use of unenhanced helical CT. Radiology 202:709–711
56. Paul JF, Blacher J, Blancher JF, Sapoval M, Safar M, Gaux JC (2000) Spontaneous renal artery dissection revealed by helical CT angiography. Eur Radiol 10:783–785
57. Waybill MM, Waybill PN (2001) Contrast media-induced nephrotoxicity: identification of patients at risk and algorithms for prevention. JVIR 12:3–9